

A 3-D FINITE ELEMENT FOR LAMINATED COMPOSITES WITH 2-D KINEMATIC CONSTRAINTS†

E. J. BARBERO

Mechanical and Aerospace Engineering, Constructed Facilities Center, West Virginia University,
Morgantown, WV 26506-6101, U.S.A.

(Received 15 August 1991)

Abstract—In this paper, a new 3-D element (3DLC) is presented for the analysis of laminated composite shells. The new element expedites the modeling process by presenting the designer with an intuitive physical interpretation for the different components of the model. The element is compatible with conventional 3-D continuum elements. It can represent arbitrarily curved shells with variable number of layers and variable thickness. Each element has a small number of degrees of freedom which facilitates its incorporation in commercial finite element codes. Aspect ratio limitations and shear locking of conventional 3-D continuum elements have been eliminated by using the kinematic constraints of layer-wise constant shear theories. The formulation and simple validation problems are presented.

1. INTRODUCTION

Modeling of laminated composites is usually performed using plate and shell elements. These elements are based on plate and shell theories which are simplifications of the three-dimensional (3-D) elasticity. The basic simplifying assumptions involve the approximation of the distribution of the displacements through the thickness of the laminate by a known function. While only kinematic assumptions are needed to develop plate theories, additional assumptions are required to deal with the curvature effects in the analysis of shells.

Most plate and shell theories assume transverse incompressibility and a state of plane stress through the thickness of the laminate. Classical plate theory (CPT) assumes that no out-of-plane shear deformation occurs through the thickness of the plate [1]. This is a very restrictive assumption for the analysis of laminated composites since they usually have very low out-of-plane shear stiffness. For this reason, CPT has been virtually abandoned in favor of first-order shear deformation theory (FSDT) for the analysis of laminated composite shells. In this refined theory, out-of-plane shear strains are assumed to be constant through the thickness of the laminate [2] and a shear correction factor is used to compute the shear strain energy accurately [3-5]. FSDT produces excellent global results (e.g., deflections, fundamental vibration frequency, etc.) but the accuracy of the stress distributions does not improve significantly over CPT. Post-processing techniques can be used to obtain refined values of the out-of-plane shear

stress components through integration of the 3-D equilibrium equations [6].

Higher-order theories have been proposed in an attempt to improve the prediction of stresses. Third-order theories are capable of representing a quadratic shear distribution through the thickness of a homogeneous shell. They satisfy the traction-free boundary conditions at the surface of the shell and there is no need for shear correction factors. All third-order theories can be derived from a common set of kinematical assumptions [7]. Higher than third-order theories have been proposed. Excellent reviews of these theories are presented by Noor [6] and Reddy [8-10]. All of these equivalent single-layer theories share a common characteristic: the assumed distribution of displacement through the thickness is not only continuous but the derivatives with respect to the thickness coordinate are also continuous. This implies that the out-of-plane shear strains are continuous across the material interfaces and, as a result of material property discontinuities, the out-of-plane stress components are discontinuous, thus violating equilibrium. The result is a limited representation of out-of-plane stresses as observed in CPT and FSDT.

The equilibrium equations can be used with all the equivalent single-layer theories to post-process the in-plane stresses and obtain a refinement of the out-of-plane stresses, but this involves considerable complexity in terms of the finite element formulation. Post-processing with the equilibrium equations requires computation of derivatives, thus requiring high-order interpolation functions to be used in the element (at least quadratic to obtain out-of-plane shear stresses and cubic to obtain transverse normal stress). An alternative solution for low-order elements is to use a finite difference scheme involving several clustered elements, but this adds significant

† Part of the material in this paper was presented at the ASCE Engineering Mechanics Speciality Conference 1991, Columbus, OH.

complexity to the program and requires an increase in the mesh refinement, which is equivalent to the use of elements with higher-order interpolation functions.

Another class of theories are based on local layer approximations and they are called layer-wise 2-D theories. These theories are based on a distribution of displacements which is continuous through the thickness of the shell but with derivatives with respect to the thickness coordinate that are not necessarily continuous at the interfaces between layers. All these theories can be derived using a displacement formulation from the generalization presented by Reddy [11]. Perhaps the best compromise between computational cost and accuracy is accomplished by layer-wise constant shear theories (LCST) like those proposed by Srinivas [12], Seide [13], Epstein *et al.*, [14, 15], Murakami [16], Hinrichsen [17], Owen [18], Reddy [19, 20] and Barbero [21, 22]. The finite element formulation of these theories result in elements with a large number of degrees of freedom (DOF) per node [20, 21] which makes the element difficult to incorporate in commercial finite element packages [23]. The physical interpretation of the DOF and a large number of stress resultants is quite difficult. So it is the imposition of boundary conditions (b.c.) and loading, since the stress resultants and displacements cannot be immediately associated with the traditional bending moments, in-plane tractions, curvatures, and in-plane displacements of the conventional theories (i.e., CPT, FSDT). The resulting elements are incompatible with other elements like 3-D solids which are usually necessary in finite element analysis (FEA). Existing finite element formulations [20, 23] are restricted to flat plates and the extension to curved shells is not simple.

Despite all the developments in the area of plate and shell theories, there is considerable interest on performing more refined FEA using 3-D elements based on continuum mechanics [24]. A number of important engineering problems (Fig. 1) are quite difficult to model accurately with plate elements for which the geometry of a solid plate is idealized by the middle surface. In bridge-and-deck monolithic construction, the intersection between thick plates and beams (Fig. 1a) can only be approximately modeled with plate elements due to the resulting overlap [25]. In folded-plate structures, intersection of plates at an angle not only introduces overlap (Fig. 1b) but also requires an additional DOF to be added to the plate element called drilling rotation. The analysis of tapered glued-laminated timber beams (Fig. 1c) is a problem of variable thickness plate. Since layers have constant thickness, the number of layers is variable and the thickness of the outer layers vanishes at certain points. Therefore, the variation of thickness cannot be simply introduced in the standard plate formulation. Ply drop-offs are discontinued layers in laminated composites (Fig. 1d). This is another problem with variable number of layers with the added

complexity that the position of the middle surface varies across the drop-off. Link elements are necessary to model ply drop-offs, lap-joints, and a variety of structures where the position of the middle surface varies from point to point.

The main advantages of conventional 3-D continuum elements are: accuracy, ease of FEA model formulation (i.e., mesh, b.c., loads, etc.), and ease of interpretation of results. The main disadvantages of conventional 3-D continuum elements are the large number of DOF involved and the aspect ratio limitation due to shear locking of fully integrated 3-D continuum elements when used for bending problems. In this paper, a new 3-D element is introduced for the analysis of laminated composite shells. The formulation is based on the fact that certain assumptions made in the plate and shell theories previously described are quite valid for a broad class of problems of moderately thick laminates. By introducing those assumptions in the formulation of a 3-D element, it is possible to obtain a less expensive 3-D element while retaining its versatility and compatibility with conventional 3-D continuum elements. This is quite important from the point of view of implementation on commercial finite element packages and use for FEA in combination with other elements already available on those packages. The proposed element is compatible with conventional 3-D continuum elements, it has a small number of DOF per node, and it produces results as accurate as conventional 3-D continuum elements for a broad range of problems. Mesh generation, imposition of b.c. and loads, and interpretation of results are identical to those used along with conventional 3-D continuum elements.

Although based on kinematical assumptions first introduced for 2-D equivalent single-layer elements, the new element is in the group of 3-D continuum-based elements according to the classification introduced by [10]. The proposed element can be considered the continuum-based implementation of LCST by analogy to the work of [26] who developed the continuum-based implementation of FSDT for laminated composites.

2. FORMULATION

The new 3-D laminated composites element (3DLC) addresses the shortcomings of higher-order plate theories and introduces additional advantages. Selected kinematical constraints are introduced on a continuum based finite element to reduce the number of DOF while retaining the desired accuracy for a class of problems, namely moderately thick laminates. The formulation uses the degenerate shell finite element concept [27]. The element can be used to model one or more layers of the laminated composite shell with arbitrary curvature and orientation. If all the all layers through the thickness of the laminate are modeled with a single element, the model

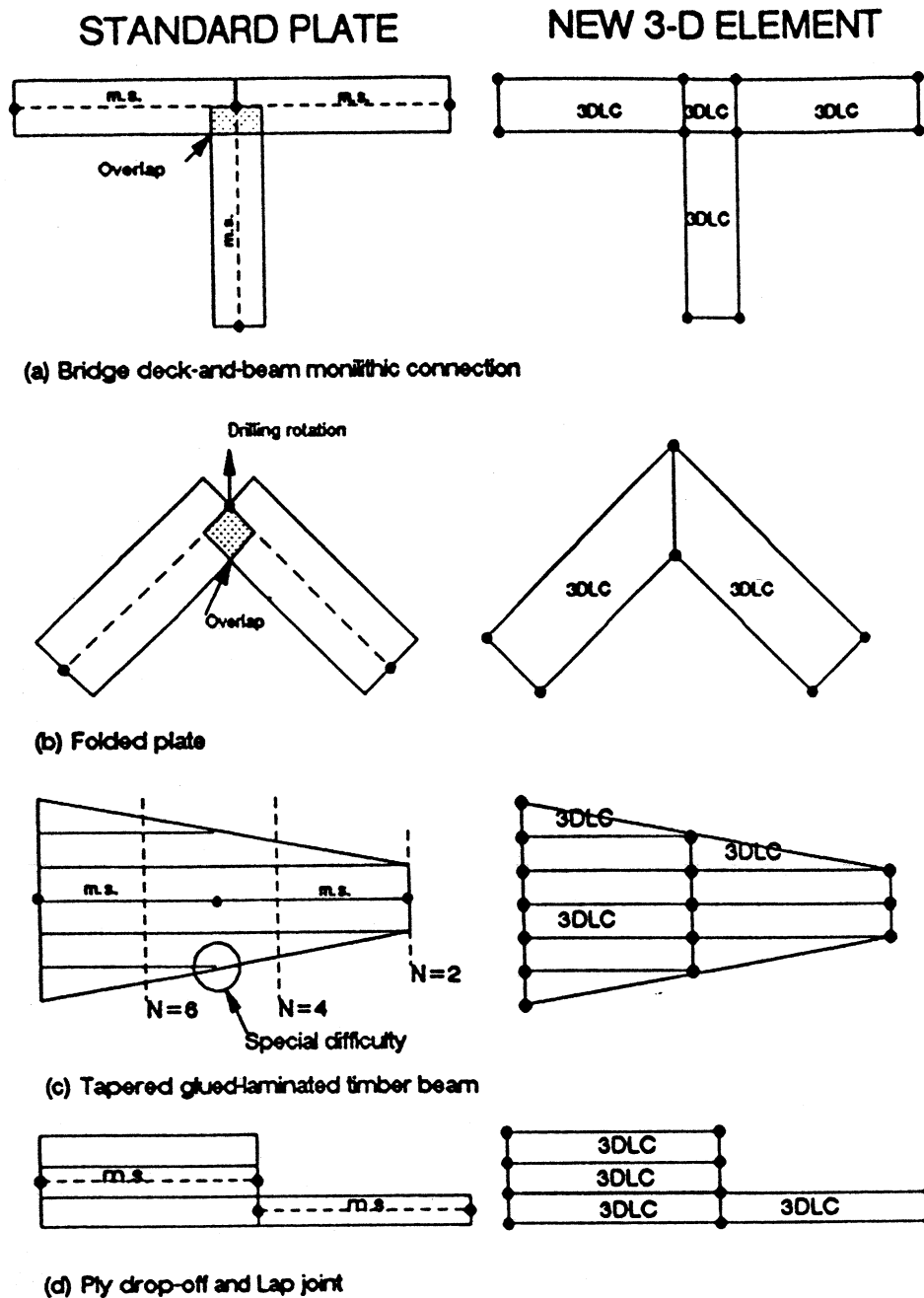


Fig. 1. Special applications for the new 3-D element compared to the approximations introduced by standard shell elements.

is equivalent to FSDT and is the least expensive and least accurate of all the possible models of a laminated composite that can be obtained with this element. If one element per layer is used, the model is equivalent to LCST and in the most accurate and expensive although less expensive than a model constructed with conventional 3-D continuum elements. Any number of elements through the thickness can be used, each representing clusters of layers. This approach leads to significant savings while retaining accuracy if an intelligent choice of clusters is made based on the stacking sequence and the

type of results desired (e.g., maximum interlaminar stresses).

Unlike plate elements based on LCST formulation, the position of the middle surface is irrelevant. Therefore, variable number of layers and thicknesses can be modeled (e.g., ply drop offs, lap joints, etc). The modeling process is very similar to the modeling using conventional 3-D continuum elements. The connectivity array is used to tie together all the elements through the thickness at a particular location and to enforce the incompressibility of the transverse normals. The new 3DLC element with this

peculiar assembly process does not interfere with the host program (e.g., ANSYS, ABAQUS) in the sense that front-width optimization routines can be used in all three directions (in-plane and through the thickness).

The quadratic element, for example, has 27 nodes. Nodes 1-18 for the variables u and v . Nodes 19-27 for the transverse deflection w only (Fig. 1). The variables u and v correspond to the in-plane displacements at the interfaces between elements (layers). The transverse deflection w is constant through the thickness. Therefore, a single global node connects to all the local w -nodes that lie on a line perpendicular to the middle surface. The quadratic element has 45 DOF. The host program calls the element subroutine for each element in turn and assembles their contribution. The host program optimizes the calling sequence to the elements to reduce the front width for frontal solvers or the band width for band solvers. The host program treats the 3DLC element as a regular 45 DOF element. The 3DLC element is in turn independent of the front with optimization algorithm, solver, etc. These characteristics are strikingly different from LCST elements which due to the large number of DOF per node are difficult to implement in commercial packages.

The nodal coordinates alone dictate the orientation of the 3DLC element in space as in standard continuum elements or degenerate shell elements. Since quadratic interpolation functions are used in this isoparametric element to model the surface geometry (Fig. 2), doubly curved shells can be modeled (Fig. 3). The element has only two DOF per node, in contrast to continuum elements that have three, plus an additional w -DOF at each location on the surface of the shell.

The displacement $\{u\} = (u, v, w)$ inside an element is given as

$$\{u\} = [N]\{\delta\}, \quad (1)$$

where $\delta = \{\delta_1\}^T, \{\delta_2\}^T, \dots, \{\delta_n\}^T$; $\{\delta_1\} = \{u_1, v_1, w_1\}^T$; n is the number of nodes, and $[N]$ is the shape function array

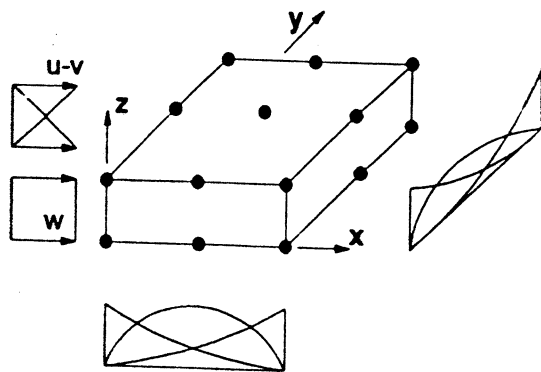


Fig. 2. Different order of interpolation through the thickness to appropriately account for the kinematic constraints.

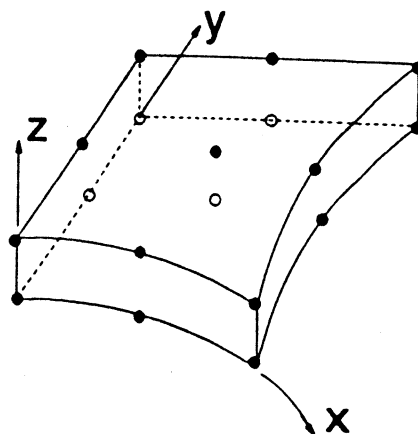


Fig. 3. Curvature as represented by the isoparametric formulation.

$$\begin{Bmatrix} u \\ v \\ w \end{Bmatrix} \begin{bmatrix} N_i & 0 & 0 \\ 0 & N_i & 0 \\ 0 & 0 & M \end{bmatrix} \begin{Bmatrix} \{\delta_i\} \\ \vdots \\ \{\delta_n\} \end{Bmatrix} \quad (2)$$

The order of the interpolation functions N_i along the two directions on the surface of the shell can be chosen independently of the order through the thickness. Linear or quadratic interpolation of the displacements (u, v) and the geometry (x, y ; Fig. 3) are commonly used. The order of approximation in the thickness direction corresponds to different kinematic assumptions in GLPT [11]. A linear variation is used in this paper (Fig. 2), but higher-order approximation functions can be easily implemented. The linear variation through the thickness of the element presents several advantages as follows:

- It reproduces FSDT kinematic assumptions when a single element is used to model the entire thickness of the laminate.
- It reproduces LCST kinematic constraints when the element is used to model a single layer of a laminate. It was demonstrated [21, 23] by comparison with exact solutions that the layer-wise linear distribution is the most efficient one. Therefore, more refined approximations through the thickness (e.g., quadratic, cubic spline) are not usually necessary. However, they can be easily implemented.
- The computational cost is reduced with respect to three-dimensional quadratic finite elements (20- or 27-node brick elements).

The order of the interpolation functions M_i along the two directions on the surface of the shell can be chosen independently of the order through the thickness. Linear or quadratic interpolation of the displacement (w) and the geometry (z ; Fig. 3) are commonly used (Fig. 2). The order of approximation in the thickness direction must be chosen according to the kinematic constraints used, reflecting different assumptions in GLPT [11]. The incompressibility of normals to the middle surface is obtained in this

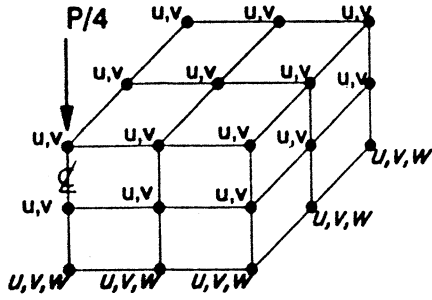


Fig. 4. Assemblage of 3DLC elements to form a laminated structure. Quarter plate, simple-supported, under concentrated load modeled by a 2×2 mesh on the x - y surface and two elements through the thickness.

paper by using a constant interpolation through the thickness (Fig. 2). Other options can be easily implemented but they increase considerably the computational cost. In this paper, the resulting element satisfies the incompressibility of normals to the middle surface of FSDT and other theories. Furthermore, the computational cost is significantly reduced since all nodes through the thickness have the same transverse deflection which can be represented as a single degree of freedom for each location on the surface of the shell (Fig. 4).

The equilibrium of the shell occupying a volume Ω is represented by the virtual work expression

$$\int_{\Omega} \{d\epsilon\}^T \{\sigma\} dv = \int_{\Omega} \{du\}^T \{q\} dv + \int_{\partial\Omega} \{du\}^T \{p\} dA. \quad (3)$$

The virtual displacement $\{du\}$ are expressed in terms of the nodal virtual displacements $\{d\delta\}$ as

$$\{du\} = [N]\{d\delta\}. \quad (4)$$

The strain tensor is written in contracted form in terms of nodal displacements $\{\delta\}$ as

$$\{\epsilon\} = [B]\{\delta\}, \quad (5)$$

where the strain matrix contains the cartesian derivatives of $[N]$

$$\begin{Bmatrix} \epsilon_x \\ \epsilon_y \\ \frac{\gamma_{xy}}{2} \end{Bmatrix} = \begin{bmatrix} N_{1,x} & 0 & 0 & \dots \\ 0 & N_{1,y} & 0 & \dots \\ N_{1,y} & N_{1,x} & 0 & \dots \end{bmatrix} \begin{Bmatrix} \delta_1 \\ \vdots \\ \delta_n \end{Bmatrix}. \quad (6)$$

The first variation of the strain tensor is

$$\{d\epsilon\} = [B]\{d\delta\}. \quad (7)$$

The left-hand side of eqn (3) represents the internal work. The external work is due to $\{du\}$ acting on the surface tractions $\{P\} = \{P_x, P_y, P_z\}$ and the body forces per unit volume $\{q\} = \{q_x, q_y, q_z\}^T$ with Ω the volume and $\partial\Omega$ the boundary of the body. The virtual

work expression [eqn (3)] is approximated by the finite element idealization as

$$\{d\delta\}^T \int_{\Omega} [B]^T \{\sigma\} dv = \{d\delta\}^T \int_{\Omega} [N]^T \{q\} dv + \{d\delta\}^T \int_{\partial\Omega} [N]^T \{p\} dA. \quad (8)$$

Since the nodal virtual displacements are arbitrary, the equilibrium equations are given by

$$\int_{\Omega} [B]^T \{\sigma\} dv = \int_{\Omega} [N]^T \{q\} dv + \int_{\partial\Omega} [N]^T \{p\} dA. \quad (9)$$

When the body volume Ω is replaced by the element volume Ω^e and the body surface $\partial\Omega$ is replaced by the element surface $\partial\Omega^e$, the element equilibrium equations are obtained

$$\int_{\Omega^e} [B]^T \{\sigma\} dv = \int_{\Omega^e} [N]^T \{q\} dv + \int_{\partial\Omega^e} [N]^T \{P\} dA. \quad (10)$$

Due to the compact support property of the interpolation functions N_i and M_i used, an assemblage of elements governed by the equilibrium as stated by eqn (10) represents the equilibrium of the entire body as stated by eqn (9).

The constitutive equations for an orthotropic material arbitrarily oriented with respect to the local coordinates is similar to the equations for a monoclinic material [28]. These equations have to be modified to introduce the plane stress assumption

$$\begin{Bmatrix} \sigma_1 \\ \sigma_2 \\ \sigma_3 \\ \sigma_4 \\ \sigma_5 \\ \sigma_6 \end{Bmatrix} = \begin{bmatrix} Q_{11} & Q_{12} & C_{13} & C_{14} & C_{26} & Q_{16} \\ Q_{12} & Q_{22} & C_{23} & C_{24} & C_{25} & Q_{26} \\ C_{13} & C_{23} & C_{33} & C_{34} & C_{35} & C_{36} \\ C_{14} & C_{24} & C_{34} & kC_{44} & kC_{45} & C_{46} \\ C_{15} & C_{25} & C_{35} & kC_{45} & kC_{55} & C_{56} \\ Q_{16} & Q_{26} & C_{36} & C_{46} & C_{56} & Q_{66} \end{bmatrix} \begin{Bmatrix} \epsilon_1 \\ \epsilon_2 \\ \epsilon_3 \\ \epsilon_4 \\ \epsilon_5 \\ \epsilon_6 \end{Bmatrix}, \quad (11)$$

where C_{ij} are the components of the 3-D stiffness matrix [28] and Q_{ij} are the components of the reduced stiffness matrix [28]. In contracted notation

$$\{\sigma\} = [D]\{\epsilon\}. \quad (12)$$

The shear correction factor k is included as required by FSDT. The need to use a shear correction factor reduces as the number of elements through the thickness of the laminate increases. This can be easily explained for the case of an isotropic plate as follows. A assemblage of 3DLC elements through the thickness represents the parabolic distribution of shear strain by a layer-wise constant approximation

when only one element is used through the thickness. Therefore, the behavior of the nine-node Lagrangian FSDT element with selective reduced integration, free of shear locking, is also present in the proposed element when several 3DLC elements are stacked through the thickness. Furthermore, Barbero and Reddy [31] successfully used selective reduced integration on their LCST element that has the same kinematics as a stack of 3DLC elements. As shown by Averil [32], the nine-node Lagrangian element with selective reduced integration does not exhibit locking as the plate (or in this paper, layer) becomes very thin. This is a remarkable advantage of 3DLC elements over conventional 3-D continuum elements with full integration.

The 3DLC element gives a very good representation of all stress components except σ_z , without the aspect ratio limitations of conventional 3-D continuum elements. When transverse stress σ_z is needed, either conventional 3-D continuum elements can be used (they are fully compatible with 3DLC elements) or further postprocessing of the 3DLC results can be done by using the third equilibrium equation

$$\frac{\partial \sigma_{xz}}{\partial x} + \frac{\partial \sigma_{yz}}{\partial y} + \frac{\partial \sigma_{zz}}{\partial z} + f_z = 0$$

5. VALIDATION

The new 3DLC element was incorporated into a standard finite element program. A few simple examples are presented to validate the program. First, a cantilever beam is modeled with two elements along the beam and one element through the thickness. The resulting model is similar to FSDT and the numerical results obtained with 3DLC and FSDT are identical. The rotations in FSDT can be related to the in-plane displacements (Fig. 6) of 3DLC as follows:

$$\beta_x = \frac{u_{i+9} - u_i}{t}, \quad \beta_y = \frac{v_{i+9} - v_i}{t},$$

where t is the thickness of the element and $i = 1, \dots, 9$. The effect of the E/G ratio is shown in Fig. 7 where it can be seen that a large value of G

simulates the classical beam theory (CBT). The beam results are obtained by setting the Poisson ratio equal to zero. The geometry of the beam is such that $s = l/h = 20$ and $w/h = 10$ where l is the length, h is the thickness, and w is the width of the beam. For a two-element mesh, the aspect ratio of the elements is 14 and no locking is observed. The material properties are $E = 30 \times 10^6$ psi and $\nu = 0.25$. The deflection at the loaded end is nondimensionalized with the CBT solution.

Next, a quarter of an orthotropic rectangular plate of side a and thickness h is modeled with a 2×2 mesh on the plane of the plate and two elements through the thickness, with a total of eight elements (Fig. 4). The aspect ratio of an element is $r = 0.707 a/h$, that for the case of thickness ratio $a/h = 80$ gives $r = 57$ and no shear locking is observed. The plate is simply supported and subjected to a concentrated load at its center (Fig. 4). The eight-element mesh has a total of 175 DOF before imposition of the boundary conditions, 150 DOF correspond to the u and v displacements at 25 locations x, y and 3 locations through the thickness. The remaining 25 DOF correspond to the transverse deflection w at the nine locations x, y on the surface of the plate. The transverse deflection w is constant through the thickness of the plate at each particular location x, y as represented by a single w -DOF at each node on the bottom surface (Fig. 4). The results are nondimensionalized with the first-term Rayleigh-Ritz approximation [2]. For homogeneous material (not laminated) the 3DLC solution coincides with the FSDT results.

The effect of the degree of orthotropicity E_1/E_2 and thickness ratio $s = a/h$ is shown in Fig. 8 for constant shear moduli $G_{12} = E_2/2$ and $G_{23} = E_2/5$. Shear deformations are correctly accounted for as shown in Fig. 9 for various values of the thickness ratio $s = a/h$ and $aE_1/E_2 = 30$. The present formulation predicts larger transverse deflections than CPT due to the effect of shear deformation that is neglected in CPT. The difference is more pronounced for small values of the thickness ratio.

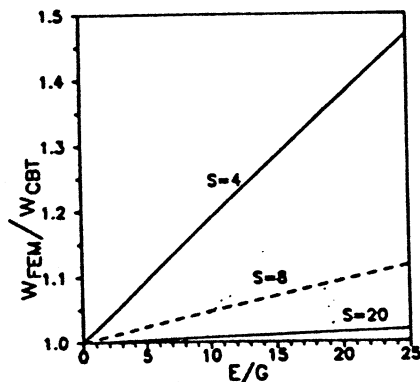


Fig. 7. Tip deflection of a cantilever isotropic beam under tip load.

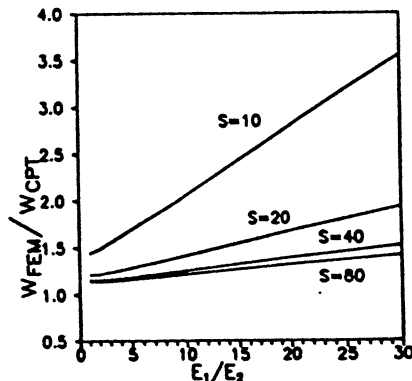


Fig. 8. Effect of the orthotropicity ratio and thickness ratio on the center deflection of an orthotropic, simple-supported, square plate under center load.

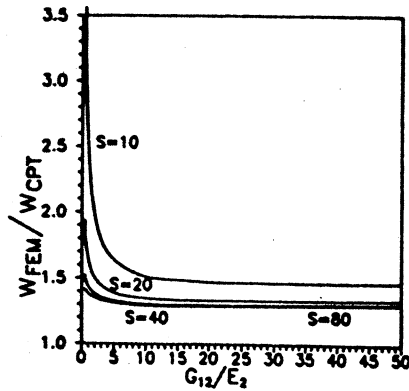


Fig. 9. Effect of the shear moduli ($G_{23} = 0.4 G_{12}$) and thickness ratio on the center deflection of an orthotropic, simply-supported, square plate under center load.

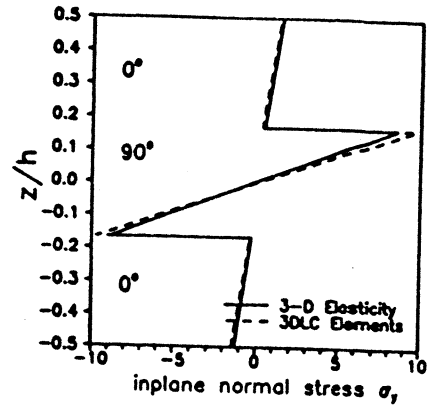


Fig. 12. Distribution through the thickness of in-plane stress σ_x in a $[0/90/0]$ square plate, simply-supported under doubly sinusoidal load.

The third example has the same geometry and boundary conditions of the previous example, but three layers of elements are used to model a $[0/90/0]$ laminate loaded by a double sinusoidal load. The exact solution to elasticity theory by Pagano [33] for $a/h = 4$ is compared to the distribution of the in-plane displacement $u(a/2, 0)$ in Fig. 10. The distri-

bution of the in-plane stresses at the nodes where they are maximum are shown in Figs 11 and 12. Interlaminar stresses obtained by postprocessing [21] are shown in Figs 13 and 14. It can be seen that the present formulation produces very good representation of the stresses through the thickness of highly anisotropic laminated plates. The 3DLC element

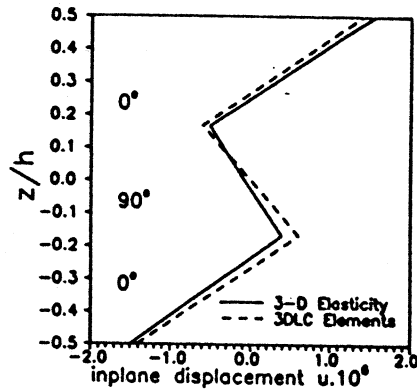


Fig. 10. Distribution through the thickness of in-plane displacement $u(a/2, 0)$ in a $[0/90/0]$ square plate, simply-supported under doubly sinusoidal load.

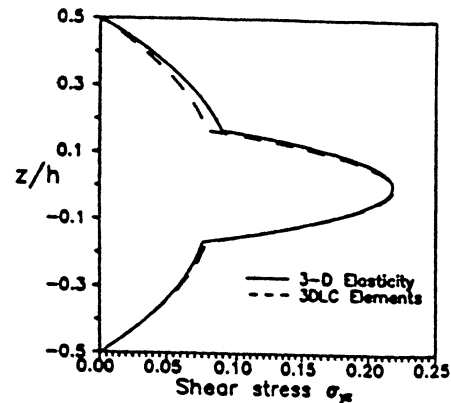


Fig. 13. Distribution through the thickness of interlaminar stress σ_{xz} in a $[0/90/0]$ square plate, simply-supported under doubly sinusoidal load.

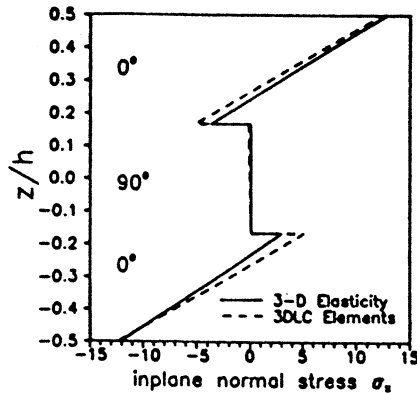


Fig. 11. Distribution through the thickness of in-plane stress σ_x in a $[0/90/0]$ square plate, simply-supported under doubly sinusoidal load.

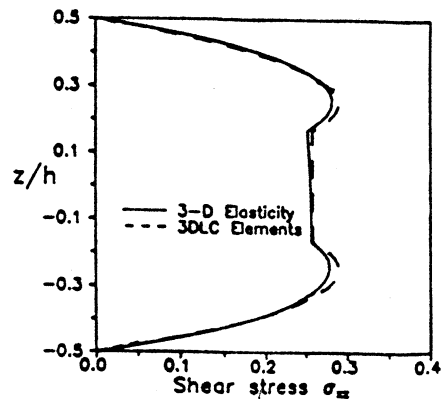


Fig. 14. Distribution through the thickness of interlaminar stress σ_{xz} in a $[0/90/0]$ square plate, simply-supported under doubly sinusoidal load.

represents accurately the laminated nature of composite shells. The results obtained from 3DLC are identical to those obtained using LCST (obtained as a special case of the generalized laminated plate theory [21]). The versatility of the new element is demonstrated with a number of examples (Fig. 1) by Ramaseshan [34].

6. CONCLUSIONS

The continuum-based implementation of layer-wise constant shear theories for laminated composites is presented. As a result, a 3-D element is developed with the advantages of laminated plate formulations and the flexibility and compatibility of 3-D continuum elements. The new element can be easily incorporated into commercial FEA packages and extended for higher-order layer-wise theories. The accuracy of the proposed element is demonstrated by standard examples used to evaluate laminated composite plate elements.

Acknowledgements—I wish to express my sincere gratitude to Dr Raphael Haftka who suggested to me the idea for the formulation presented in this paper. My appreciation to Dr J. N. Reddy who contributed immensely to this area of research. The help of A. S. Ramaseshan with the computations and constructive suggestions of Dr Elio Sacco are also acknowledged.

REFERENCES

1. A. C. Ugural, *Stresses in Plates and Shells*. McGraw-Hill, New York (1981).
2. J. N. Reddy, *Energy and Variational Methods in Applied Mechanics*. John Wiley, New York (1984).
3. J. M. Whitney, Shear correction factors for orthotropic laminates under static load. *J. Appl. Mech.* **40**, 302–304 (1973).
4. C. W. Bert, Simplified analysis of static shear factors for beams of nonhomogeneous cross section. *J. Comp. Mater.* **7**, 525–529 (1973).
5. A. K. Noor and W. S. Burton, Stress and free vibration analysis of multilayered composite plates. *Comput. Struct.* **11**, No. 2 (1989).
6. A. K. Noor and W. S. Burton, Assessment of shear deformation theories for multilayered composite plates. *Appl. Mech. Rev.* **42**, 1–12 (1989).
7. J. N. Reddy, A general non-linear third-order theory of plates with moderate thickness. *Int. J. Non-linear Mech.* **25**, 677–686 (1990).
8. J. N. Reddy and K. Chandrashekhara, Recent advances in the nonlinear analysis of laminated composite plates and shells. *Shock Vibr. Digest* **19**, 3–9 (1987).
9. J. N. Reddy, On the generalization of displacement-based laminate theories. *Appl. Mech. Rev.* **42**, S213–S222 (1989).
10. J. N. Reddy, On refined computational models of composite laminates. *Int. J. Numer. Meth. Engng* **27**, 361–382 (1989).
11. J. N. Reddy, A generalization of two-dimensional theories of laminated plates. *Commun. Appl. Numer. Meth.* **3**, 113–180 (1987).
12. S. Srinivas, Refined analysis of composite laminates. *J. Sound Vibr.* **30**, 495–507 (1973).
13. P. Seide, An improved approximate theory for the bending of laminated plates. *Mechanics Today* **5**, 451–466 (1980).
14. M. Epstein and P. G. Glockner, Nonlinear analysis of multilayered shells. *Int. J. Solids Struct.* **13**, 1081–1089 (1977).
15. M. Epstein and H. P. Huttelmaier, A finite element formulation for multilayered and thick plates. *Comput. Struct.* **16**, 645–650 (1983).
16. H. Murakami, Laminated composite plate theories with improved inplane responses. ASME Pressure Vessels and Piping Conference, pp. 257–263 (1984).
17. R. L. Hinrichsen and A. N. Palazotto, The nonlinear finite element analysis of thick composite plates using a cube spline function. *AIAA Jnl* **24**, 1836–1842 (1986).
18. D. R. J. Owen and Z. H. Li, A refined analysis of laminated plates by finite element displacement methods—I. Fundamentals and static analysis; II. Vibrations and stability. *Comput. Struct.* **26**, 907–923 (1987).
19. J. N. Reddy, A generalization of two-dimensional theories of laminated plates. *Commun. Appl. Numer. Meth.* **3**, 113–180 (1987).
20. J. N. Reddy, E. J. Barbero and J. L. Teply, A plate bending element based on a generalized laminate plate theory. *Int. J. Numer. Meth. Engng* **28**, 2275–2292 (1989).
21. E. J. Barbero, On a generalized laminate theory with application to bending, vibration and delamination buckling in composite laminates. Ph.D. dissertation, Virginia Polytechnic Institute and State University, Blacksburg, VA (1989).
22. E. J. Barbero, J. N. Reddy and J. L. Teply, General two-dimensional theory of laminated cylindrical shells. *AIAA Jnl* **28**, 544–553 (1990).
23. E. J. Barbero, J. N. Reddy and J. L. Teply, A plate bending element based on the generalized laminate theory: implementation into ABAQUS computer program. CCMS-89-08, Virginia Polytechnic Institute and State University, Blacksburg, VA (1989).
24. M. Vidussoni, Global-local finite element analysis of laminated composites. Thesis, Virginia Polytechnic Institute and State University, Blacksburg, VA (1988).
25. S. F. Ng, M. S. Cheung and Z. Bingzhang, Finite strip method for analysis of structures with material nonlinearity. *ASCE J. Struct. Engng* **117**, 489–500 (1991).
26. W. C. Chao, Analysis of laminated composite shells using a degenerated 3-D element. *Int. J. Numer. Meth. Engng* **20**, 1991–2007 (1984).
27. S. Ahmad, Analysis of thick and thin shell structures by curved finite elements. *Int. J. Numer. Meth. Engng* **2**, 419–451 (1970).
28. R. N. Jones, *Mechanics of Composite Materials*. Hemisphere, New York (1975).
29. R. A. Chaudhuri, An equilibrium method for the prediction of transverse shear stresses in a thick laminated plate. *Comput. Struct.* **23**, 139–146 (1986).
30. R. D. Cook, *Concepts and Applications of Finite Element Analysis*, 2nd Edn. John Wiley, New York (1974).
31. E. J. Barbero and J. N. Reddy, An accurate determination of stresses in thick laminates using a generalized plate theory. *Int. J. Numer. Meth. Engng* **29**, 1–14 (1990).
32. R. C. Averil, On the behavior of shear deformable plate elements. Thesis, Virginia Polytechnic Institute and State University, Blacksburg, VA (1989).
33. N. J. Pagano, Exact solutions for rectangular bidirectional composites and sandwich plates. *J. Comp. Mater.* **4**, 20–35 (1970).
34. A. S. Ramaseshan, Validation and application of a 3-D laminated composite element. Thesis, West Virginia University, Morgantown, WV 26506 (1991).